FEBS Letters 580 (2006) 455–462

Mammalian mitochondrial nitric oxide synthase: Characterization of a novel candidate

Tomasz Zemojtel[a,b,*,1], Mateusz Kolanczyk[b,c,*,1], Nadine Kossler[c], Sigmar Stricker[c], Rudi Lurz[d], Ivan Mikula[e], Marlena Duchniewicz[b], Markus Schuelke[f], Pedram Ghafourifar[g], Pavel Martasek[e], Martin Vingron[a], Stefan Mundlos[c]

[a] *Department of Computational Molecular Biology, Max Planck Institute for Molecular Genetics, Ihnestrasse 73, D-14195 Berlin, Germany*
[b] *In silico Miners, Chopina 13/10, 81-782 Sopot, Poland*
[c] *Department of Development and Disease, Max Planck Institute for Molecular Genetics, Ihnestrasse 73, D-14195 Berlin, Germany*
[d] *Microscopy Group, Max Planck Institute for Molecular Genetics, Ihnestrasse 73, D-14195 Berlin, Germany*
[e] *Department of Pediatrics, Center of Applied Genomics, First School of Medicine, Charles University, 121 09 Prague, Czech Republic*
[f] *Department of Neuropediatrics, Charite, University Medical Center, Berlin, Germany*
[g] *Department of Pharmacology, Joan C. Edwards School of Medicine, Marshall University, Huntington, WV 25704, USA*

Received 24 October 2005; revised 5 December 2005; accepted 13 December 2005

Available online 20 December 2005

Edited by Robert Barouki

Abstract **Recently a novel family of putative nitric oxide synthases, with AtNOS1, the plant member implicated in NO production, has been described. Here we present experimental evidence that a mammalian ortholog of AtNOS1 protein functions in the cellular context of mitochondria. The expression data suggest that a candidate for mammalian mitochondrial nitric oxide synthase contributes to multiple physiological processes during embryogenesis, which may include roles in liver haematopoesis and bone development.**

Keywords: Mitochondrial nitric oxide synthase; AtNOS1 ortholog

1. Introduction

In mammals, three highly homologous isoforms of nitric oxide synthase (NOS) catalyze oxidation of L-arginine to nitric oxide and L-citruline. NOS enzyme is composed of a catalytic heme-containing oxygenase domain (NOSoxy) [1] and a sulfite reductase flavoprotein-like domain (NOSred) [2,3]. Both domains are linked via a helical CaM-binding peptide [4,5]. Interestingly, a gene homologous to the NOSoxy domain was identified in a number of prokaryotes [3,6]. Yet a homologue of the mammalian NOS gene is absent from up-to-date sequenced genomes of plants and single cellular eukaryotes (i.e., yeast).

Intriguingly, recent reports hinted a possibility that a novel NO source is at play. In the first, the authors described a *Helix pomatia* (snail) gene that, when over-expressed in *Escherichia coli*, increases NOS activity in crude extracts [7]. Subsequently, its plant ortholog, AtNOS1, was found to be associated with arginine-dependent NO production in *Arabidopsis* [8]. This find triggered the description of a novel family of putative NOS with members in virtually all organisms from bacteria to humans [9]. Curiously, these proteins display no homology to already known animal NOSs and contain a centrally positioned GTP-binding domain.

As the first steps in our ongoing effort to functionally characterize mammalian members of this peculiar protein family, we cloned the mouse AtNOS1 ortholog, mAtNOS1, and analysed its subcellular localization and expression domain.

2. Materials and methods

2.1. Protein constructs

mAtNOS1 coding sequence (693 a.a.) was RT-PCR derived on a template of RZPD cDNA clone (GI:16877844) and subcloned into pcDNA3.1 vector.

Primer sequences used for cloning a full length ORF, Δ(1–26)mAtNOS1-V5 and Δ(1–56)mAtNOS1-V5 N-terminus deletion mutants of mAtNOS1, and (1–60)mAtNOS1-EGFP fusion protein are listed in the method section of Supplementary Information.

2.2. Cell lines and cell transfection

COS-1 and NIH3T3 cells were grown on Dulbecco's modified Eagle's high glucose medium (DMEM) supplemented with 5% fetal calf serum (FCS), penicillin (100 U/ml) and streptomycin (100 μg/ml). Transfection was done using PolyFect (Qiagen).

2.3. Immunofluorescence and microscopy

COS-1 and NIH3T3 cells were grown on coverslips and fixed 48 h after transfection with 4% paraformaldehyde for 10 min at room temperature. The cells were permeabilized with 0.2% Triton X-100 in PBS and incubated with primary antibody diluted in PBS, 10% FCS and 0.05% NaN_3 for 1 h at room temperature. For the MitoTracker® Red CM-H2Xros staining, the cells were fixed and permeabilized with ice-cold methanol for 10 min at −20 °C. Secondary antibodies were diluted in PBS, 10% FCS and 0.05% NaN_3 and incubated on coverslips for 1 h at room temperature. The coverslips were mounted on slides in Fluoromount-G (Electron Microscopy Sciences). The samples were examined with a fluorescence microscope Axiovert-200 (Zeiss) and processed with deconvolution algorithm using Axio Vision 4.3 software.

*Corresponding authors. Fax: +49 30 8413 1152.
E-mail addresses: zemojtel@molgen.mpg.de (T. Zemojtel), kolanshy@molgen.mpg.de (M. Kolanczyk).

[1] Both authors contributed equally.

Abbreviations: mAtNOS1, mouse ortholog of AtNOS1; hAtNOS1, human ortholog of AtNOS1; mtNOS, mitochondrial nitric oxide synthase; NADPH, nicotinamide adenine dinucleotide

0014-5793/$32.00
doi:10.1016/j.febslet.2005.12.038

For electron microscopy, the cells were fixed with 4% formaldehyde and 0.2% glutaraldehyde for 1 h, dehydrated in an ethanol series and embedded in LR-White or LR-Gold (London Resin Company). For embedding in LR-Gold Resin, cells were grown on poly-lysine-coated Thermanox coverslips (13 mm diameter; Nunc, Naperville, IL). For embedding in LR-White Resin, cells grown in 10 cm culture dish were fixed and harvested with cell scraper. Post-embedded immunogold labelling was performed using the rabbit-anti-V5 antibody (1:50) followed by secondary antibody conjugated with 10 nm gold (1:100; British Bio Cell). The samples were viewed in a Philips CM 100 electron microscope.

2.4. Cell fractionation and Western blotting

Citrate synthase (CS) and lactate dehydrogenase (LDH) activities in the cytosolic as well as in the mitochondrial fraction were measured as previously described [10,11]. Subcellular fractionation of COS-1 cells was performed using cytosol/mitochondria fractionation kit (Oncogene) according to the following protocol. Cells were grown as adherent cultures in 75 cm^2 tissue culture bottles with DMEM supplemented with 10% FCS. At near confluence the cells were harvested by trypsination and washed twice with ice-cold extraction buffer (10 mM HEPES, pH 7.5, 200 mM mannitol, 70 mM sucrose, 1 mM EGTA). This yielded approximately 10^7 cells. From here all steps were performed at 4 °C. The cell pellet was re-suspended in 2 ml extraction buffer supplemented with 2 mg/ml albumin and the cells were disrupted by eight slow up- and down strokes through a tightly fitting Teflon pestle rotating in a Potter-Elevhjem homogenizer at 500 rpm. The homogenate was transferred into 2 ml Eppendorf tubes and centrifuged at $600 \times g$ for 5 min to remove the cell nuclei. The supernatant was then transferred into a new tube and centrifuged at $11\,000 \times g$ for 10 min. The supernatant was carefully removed and collected as the cytosolic fraction and the remaining mitochondrial pellet was re-suspended in storage buffer (10 mM HEPES, pH 7.4, 250 mM sucrose, 1 mM ATP, 0.08 mM ADP, 5 mM sodium succinate, 2 mM K_2HPO_4, 1 mM DTT).

Finally, the protein content of the cytosolic and of the mitochondrial fraction were measured with a standard BCA assay. Proteins in cytosolic and mitochondrial fractions were solubilized in Laemmli buffer, resolved on 10% polyacrylamide gel and transferred onto PVDF (Amersham). Immunoblots were developed using ECL detection system (Amersham).

The following antibodies were used in immunofluorescence and/or WB analyses: mouse anti-V5 IgG2a (Invitrogen); goat anti-mouse IgG Peroxidase Conjugated (Calbiochem); goat anti-rabbit IgG Peroxidase Conjugated (Oncogene); rabbit anti-Prohibitin IgG polyclonal ab2996 (Abcam); mouse anti cytochrome *C* IgG clone 7H8.2C12 (Pharmingen); goat anti-mouse IgG Alexa Flour-546 (Molecular Probes); goat anti-mouse IgG Alexa Flour-488 (Molecular Probes); rabbit anti-Actin A2066 (Sigma).

2.5. In situ hybridization

Section in situ hybridization on frozen E12.5 embryos was done with digoxygenin labelled rRNA probe according to protocols of the GenePaint™ system (Tecan) [12]. Section in situ hybridization on E14.5 embryos was performed on paraffin embedded tissue using ^{33}P labelled cRNA-probes as described previously [13].

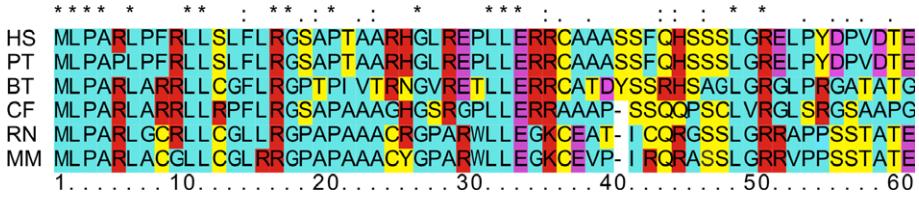

Fig. 1. Alignment of the N-terminal sequences of mammalian AtNOS1 orthologs. HS, *Homo sapiens* (GI: 14150078); PT, *Pan troglodytes*; BT, *Bos taurus*; CF, *Canis familiaris*; RN, *Rattus norvegicus* (GI: 34876747); MM, *Mus musculus* (GI: 9790049). Residues in blue, non-polar; yellow, uncharged polar; red, charged polar; purple, negatively charged.

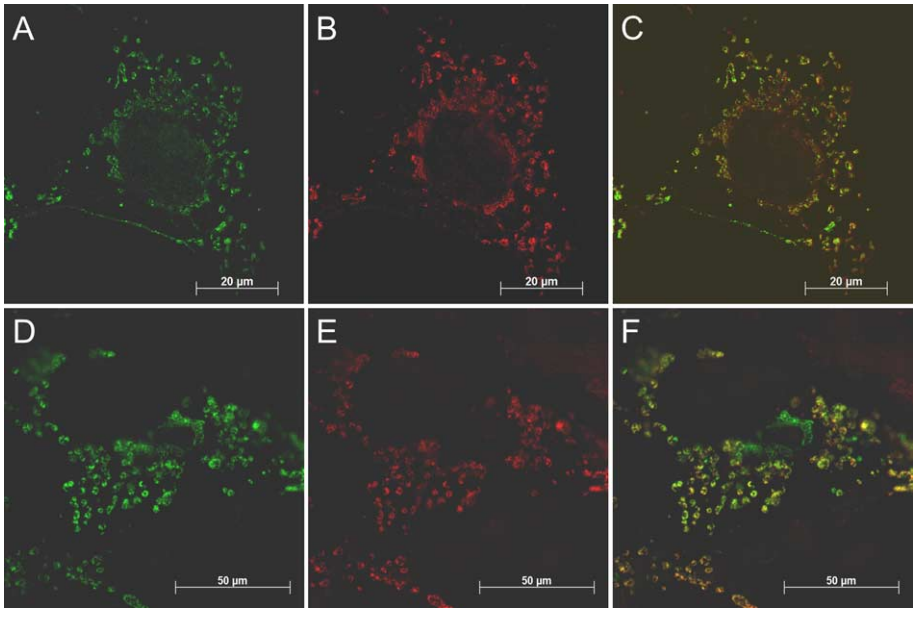

Fig. 2. Mitochondrial localization of mAtNOS1. COS1 cells, transiently transfected with V5-His-tagged mAtNOS1 (A–F) cultured for 48 h and immunostained with mouse anti-V5 antibody (Invitrogen) and rabbit anti-Prohibitin antibody – ab2996 (Abcam) followed by anti mouse-IgG Alexa Fluor 488 and anti rabbit-IgG Alexa Fluor 546 conjugated secondary antibodies, respectively (A–C). Alternatively, mitochondria were stained with MitoTracker® Red CM-H2Xros (D–F).

2.6. Northern blotting analysis

Total RNA was isolated from fresh homogenized tissue samples using Total RNA isolation kit (AABiot, Gdynia, Poland) and electrophoresed (10 μg/lane) through 1% formaldehyde gel. RNA was transferred to Hybond N^+ membrane (Amersham) and UV cross-linked with UV-Stratalinker (Stratagene). The *mAtNOS1* probe comprising the PCR-derived full coding sequence region was labelled with [^{32}P] dCTP using Megaprime DNA labelling system (Amersham Biosciences).

3. Results and discussion

3.1. N-terminal signalling peptide

Initial analyses of the putative NOS family showed that eukaryotic sequences, when compared to bacterial, are longer in their N-terminus [9]. Our closer examination of the N-terminal regions of mammalian sequences revealed enrichment in charged residues, particularly arginines (Fig. 1). The latter is a common feature of leader peptides [14]. To investigate this matter further, we employed a tool, Target-*P*, that predicts the subcellular location of eukaryotic proteins [15]. Strikingly, all mammalian N-terminal peptides were classified, with a high probability (i.e., for the human sequence: Target-*P* score >0.9, RC = 1), as the mitochondrial targeting peptides. With those matters settled, we aimed for experimental validation of the generated predictions.

3.2. Subcellular localization of mAtNOS1

First, we constructed a fusion gene, mAtNOS1-V5, in which His-V5 tag was attached at the C-terminus of mAtNOS1 coding sequence (693 a.a.). This allowed us to examine the subcellular localization of mAtNOS1-V5 in transiently transfected COS-1 and NIH3T3 cells. Immunolabelling with anti V5-antibody revealed a mitochondrial pattern of distribution, subsequently confirmed by co-immunodetection with anti-Prohibitin antibody and staining with a mitochondrial marker MitoTracker® (Fig. 2). Having established that, we further explored the localization of mAtNOS-V5 by immune-gold electron microscopy. Fig. 3 clearly shows that the protein localizes to the inner-mitochondria compartment. Since colloidal gold particles were frequently found within the mitochondria cristae (Fig. 3B and C), we find it highly plausible that the inner mitochondria membrane is the primary site of mAtNOS1 localization.

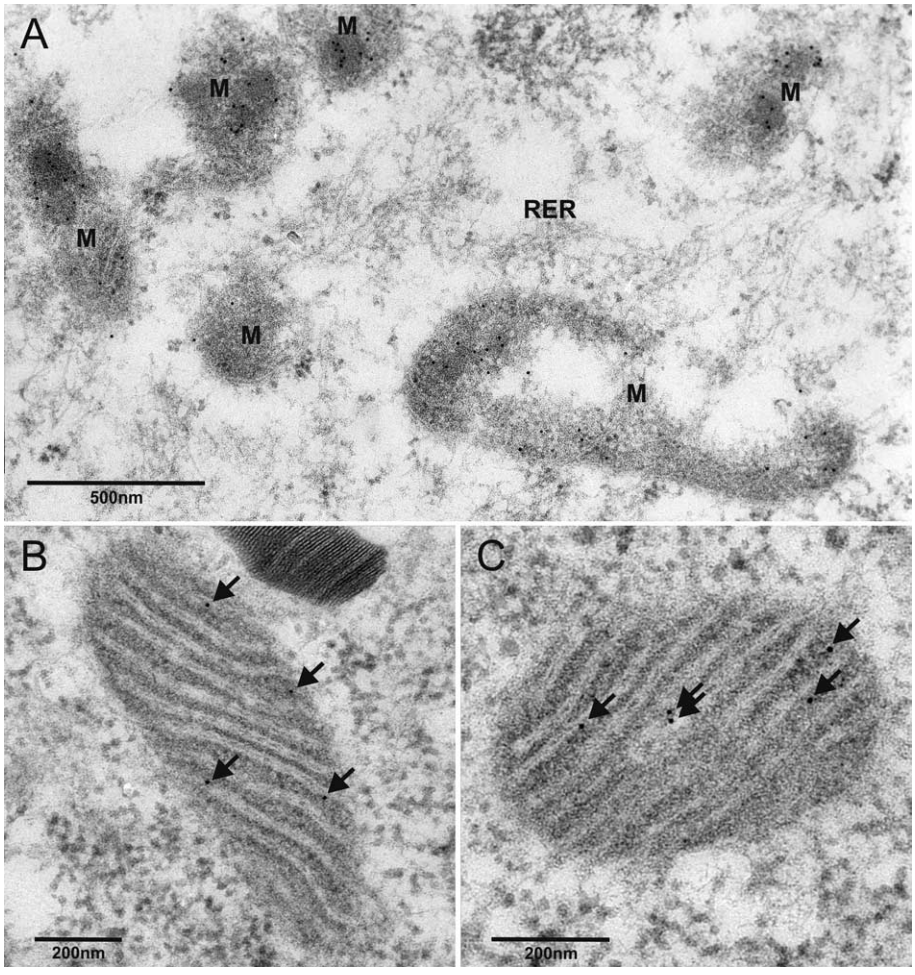

Fig. 3. mAtNOS1 exhibits intramitochondrial localization. COS1 cells, transiently transfected with V5-His-tagged mAtNOS1, cultured for 48 h and processed for EM-immunostaining with LR white resin (A) or LR gold resin (B,C) – see Section 2 for a detailed protocol. Cells were immunostained with mouse anti-V5 antibody as described in Section 2. Colloidal gold particles are frequently associated with the cristae membranes of mitochondria (B,C; arrows). Only very few particles, corresponding to the background, are present outside mitochondria (A). M – mitochondria; RER – raw endoplasmic reticulum.

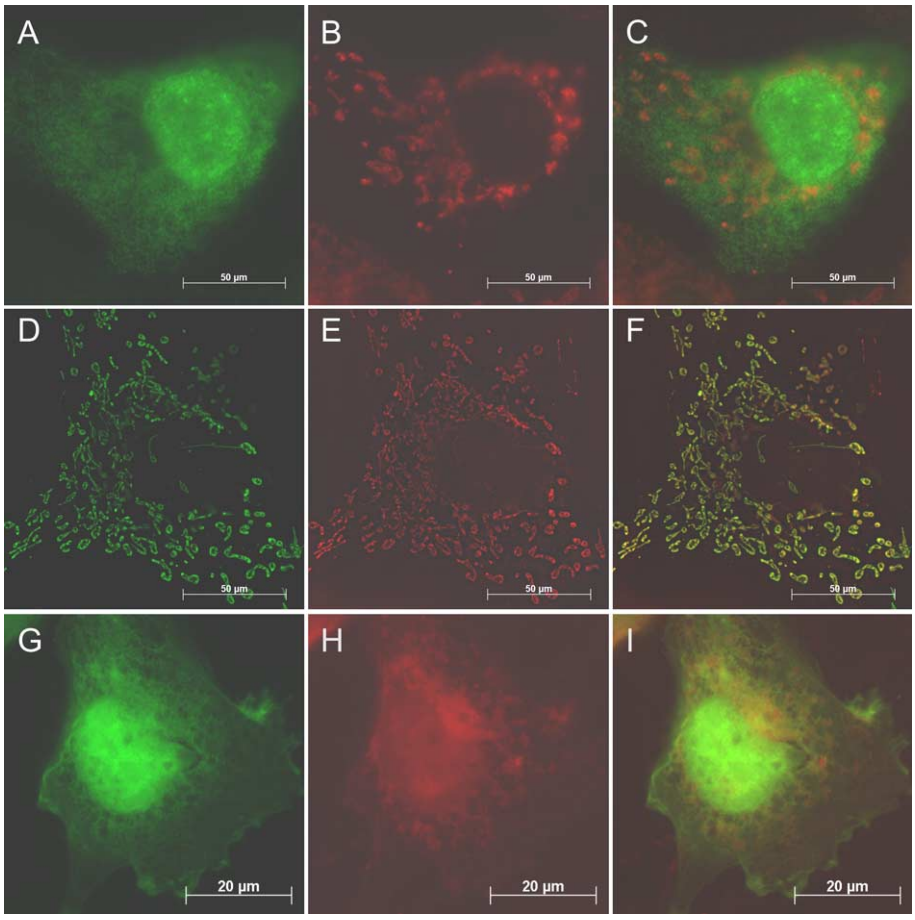

Fig. 4. The N-terminus of mAtNOS1 contains a mitochondrial targeting signal. COS1 cells, transiently transfected with Δ(1–26)mAtNOS1-V5 (A–C), (1–60)mAtNOS1-EGFP (D–F) and EGFP (G–I), cultured for 48 h and stained with mitochondria specific marker MitoTracker® Red CM-H2Xros (A–I). (A–C) Green fluorescence from immunostaining with mouse anti-V5 antibody (Invitrogen) and anti mouse-IgG Alexa Fluor 488. (D–I) Green fluorescence from EGFP.

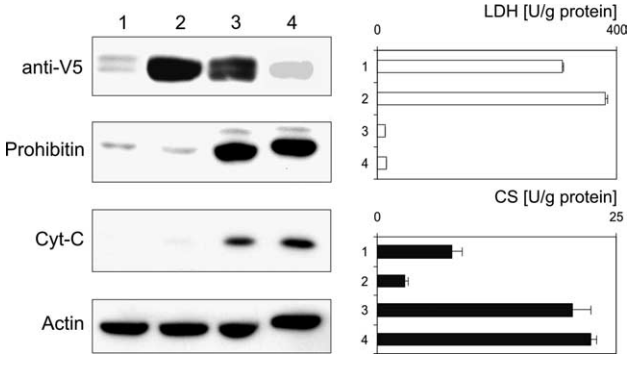

Fig. 5. N-terminus dependent enrichment of mAtNOS1 in mitochondria. Cytosolic (lanes 1 and 2) and mitochondrial (lanes 3 and 4) distribution of the V5-His-tagged mAtNOS1 protein was analyzed by Western blotting. COS1 cells were transiently transfected with mAtNOS1 (lanes 1 and 3), and Δ(1–56)mAtNOS1-V5 (lanes 2 and 4) constructs and fractionated into mitochondria-enriched and cytosolic fractions using cytosol/mitochondria fractionation kit (Oncogene Research Products). Western blots were followed by immunodetection with antibodies against V5 epitope, prohibitin, cytochrome *C* and actin. Activity (in U/g of protein) of cytosolic LDH and mitochondrial CS in each fraction is presented as mean ± S.D.

3.3. The amino terminus of mAtNOS1 contains a mitochondrial targeting signal

In order to test if the N-terminal sequence encodes a mitochondrial targeting peptide, we constructed deletion mutants devoid of 26 and 56 amino acids at the N-terminus, Δ(1–26)mAtNOS1-V5 and Δ(1–56)mAtNOS1-V5, respectively. Both mutant proteins no longer co-localized with MitoTracker® and exhibited a diffuse distribution in the transient transfected COS1 and 3T3NIH cells (Fig. 4, Fig. S1, result for Δ(1–56)mAtNOS1-V5 not shown). This notion is further supported by a fractionation experiment, in which a significant enrichment of Δ(1–26)mAtNOS1-V5 and Δ(1–56)mAtNOS1-V5 mutants was observed in the cytoslic fractions, as compared to the mitochondrial fractions of COS1 cells (Fig. 5, results for Δ(1–26)mAtNOS1-V5 not shown).

In order to further study the involvement of N-terminus in the subcellular localization of the protein, we transfected COS-1 cells with a construct encoding a fusion between amino acids 1–60 of mAtNOS1 and enhanced green fluorescent protein (EGFP). Markedly, (1–60)mAtNOS1-EGFP fusion gene co-localized with MitoTracker® in COS1 and NIH3T3 cells (Fig. 4, Fig. S1). Thus, our results indicate that the first 60 amino acids of mAtNOS1 contain a mitochondrial targeting signal that is necessary and sufficient for import into mitochondria.

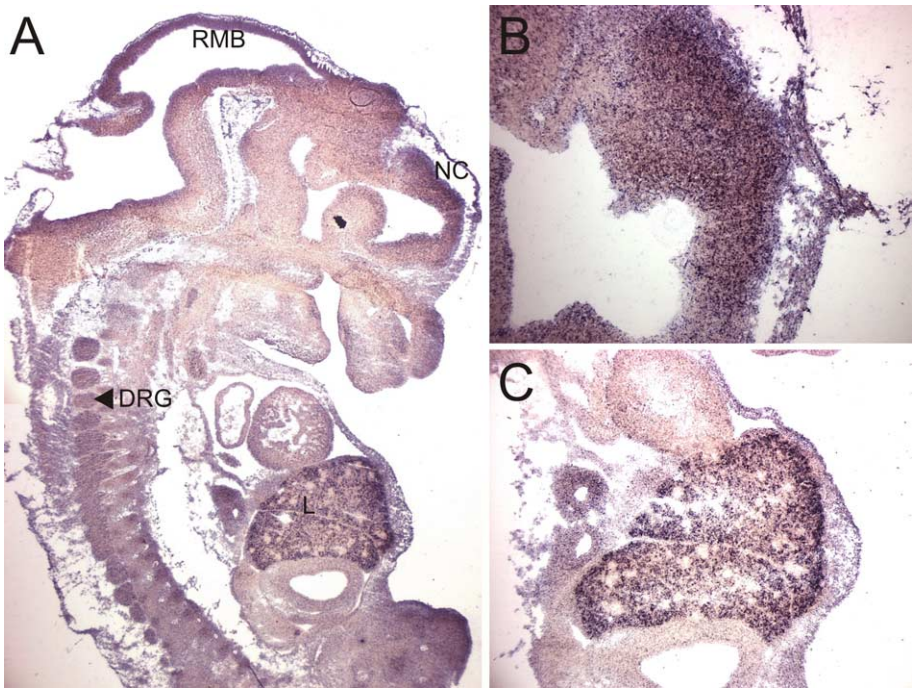

Fig. 6. Expression of mAtNOS1 at E12.5. In situ hybridization of digoxygenin labeled probe on OCT frozen parasagittal sections of E12.5 wild-type embryo. Expression is detected in the developing central and peripheral nervous system as well as in the liver. Magnified areas of intense expression in the neopallial cortex and liver, B and C, respectively. Dorsal root ganglia (DRG), roof of midbrain (RMB), liver (L), neopallial cortex (NC).

3.4. Expression pattern of mouse AtNOS1 ortholog

Next, we analysed the embryonic expression pattern of mAtNOS1 gene. Whole-mount in situ hybridization experiments at E10.5 revealed a weak, but widespread expression of mAtNOS1 (data not shown). In situ hybridization on frozen mouse embryonic sections at later stage of gestation, E12.5, showed prominent expression of mAtNOS1 in the liver (Fig. 6). The latter may be indicative of its function in embryonic liver haematopoesis. In addition, mAtNOS1 was detected in the developing CNS and dorsal root ganglia. Interestingly, at E14.5 mAtNOS1 expression was intensified in the bone (Fig. 7). On the coronary sections of E14.5 mouse embryo, expression was detected in the ossified parts of the ribs, whereas no expression could be seen in the cartilaginous parts. Also at the longitudinal sections through E14.5 embryo humerus, mAtNOS1 expression was observed in the ossification zone but not in the cartilage, supporting the notion that bone cells and not chondrocytes express mAtNOS1 (Supp. Fig. 2). In summary, in situ hybridization data is suggestive of a role for mAtNOS1 in development of neural, haematopoietic and bone organ systems.

We also explored the question of whether the gene is expressed in established bone cell lines. Interestingly, Northern blot detected mAtNOS1 mRNA in primary calvaria osteoblasts, as well as established stroma (ST-2), pre-osteoblastic (MC3T3-E1), osteocyte (MLOY4) and multipotent mesenchymal (C3H10T1/2) cell lines (Fig. 8). Lastly, we probed total RNA from adult mouse organs for mAtNOS1 expression. Northern blot revealed that the gene was expressed in the organs associated with high mito chondria content, like testes, heart, liver, brain and thymus (Fig. 8).

4. Summary and outlook

We showed that mouse AtNOS1 ortholog, mAtNOS1, localizes to mitochondria. It can be expected, on the bases of a high sequence similarity in the regions corresponding to the N-terminal targeting peptide (Fig. 1), that all of mammalian AtNOS1 orthologs are mitochondrial proteins. Moreover, according to Target-*P* predictions, *Arabidopsis* sequence, AtNOS1, is also a mitochondrial protein (Target-*P* score of ~0.8), suggesting a conservation of the subcellular localization among eukaryota. Indeed, while the present study was in review, Guo et al. reported that *Arabidopsis* AtNOS1 protein, a like its mammalian ortholog, mAtNOS1, is also targeted to mitochondria [16]. Moreover, the mitochondria isolated from the AtNOS1 mutant plant (AtNOS1 −/−) were defective in L-Arg based NO production. Elevated levels of hydrogen peroxide, superoxide anion, oxidized lipid, and oxidized proteins were detected in the AtNOS1 −/− plant.

This set of findings is especially interesting in the light of the ongoing debate on existence of a mammalian mitochondrial NOS (mtNOS) [17–19]. mtNOS has been described as an L-arginine and Ca^{2+} dependent enzyme that is associated with the mitochondrial inner membrane and regulates mitochondrial respiration via produced NO [20–23]. It is note worthy that NO has been shown to stimulate biogenesis of respiratory functional and metabolically active mitochondria [24]. Subsequently, multiple groups, by utilizing antibodies raised against the nicotinamide adenine dinucleotide (NADPH)-binding C-terminus of classical NOSs, identified eNOS [21,25,26], iNOS [27] and nNOS [28–30] as mitochondrial NOS (for a detailed discussion see reviews [17–19]). Still, others did not detect nNOS nor iNOS in the mitochondria,

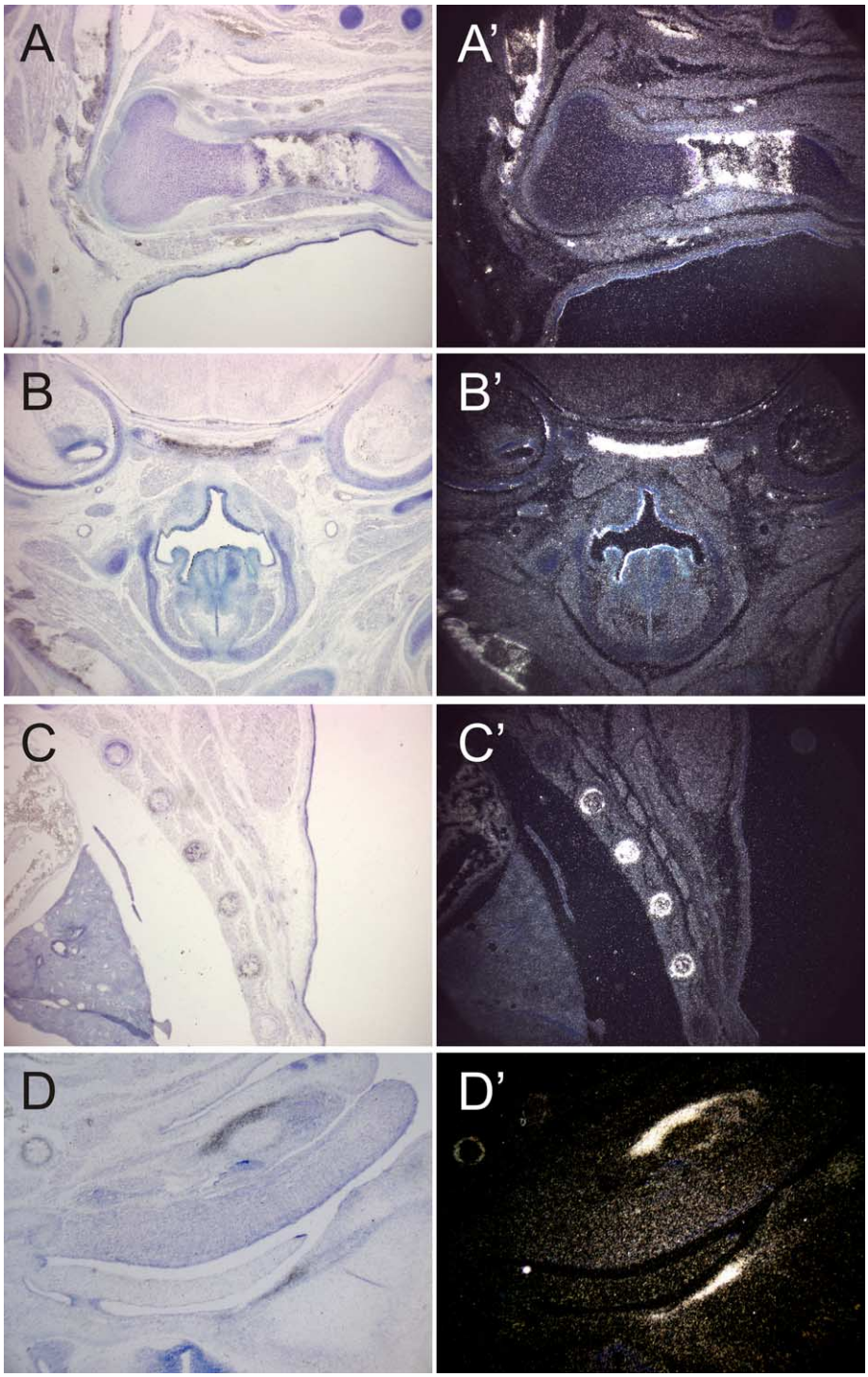

Fig. 7. Expression of mAtNOS1 at E14.5. In situ hybridization on coronary and parasagittal paraffin sections of E14.5 wild-type embryos. Left panel shows the bright field image, right panel the dark field. mAtNOS1 expression is seen in the ossification zone within the shaft of the humerus (A–A′), the primordium of basioccipital bone (B–B′), the rib primordia (C–C′) and in primordia of incisor teeth (D–D′).

and also excluded eNOS as a source of NO in this organelle [31].

Are mammalian AtNOS1 orthologs the long-sought mtNOS? To date, the NOS activity has been documented for *Arabidopsis* AtNOS1 protein [8]. However, for the latter, a catalytic mechanism of NO production is still not known. Interestingly, sequences belonging to the novel, putative NOS family, including AtNOS1 member, contain within their N-terminus a treble clef finger-like motif CxxC–x(26–34)–CxxC [9] known to be involved in metal binding [32]. The latter may constitute an active site or electron acceptor site. The study on Arabidopsis AtNOS1 protein revealed that NOS activity was dependent on NADPH [8]. Intriguingly, the NADPH-binding site appears to be absent in AtNOS1 sequence. A pos-

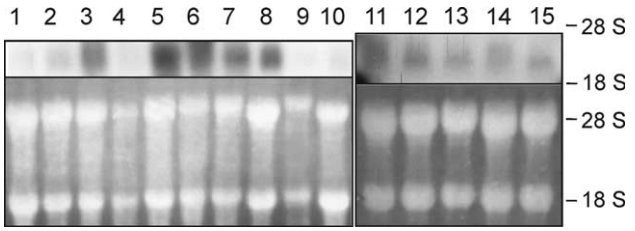

Fig. 8. Northern blot analysis of mAtNOS1 in adult mouse organs and mesenchymal, stromal, osteoblastic and osteocytic cell lines. The 28S and 18S rRNAs are indicated on the right side. Upper panel – hybridization with mAtNOS1 specific probe. Samples are in the following order: placenta (1), liver (2), kidney (3), lungs (4), testes (5), heart (6), brain (7), thymus (8), spleen (9) and stomach (10), primary calvaria osteoblasts (11), ST2 – stroma cell line (12), MC3T3 pre-osteoblastic cell line (13), C3H10T1/2 multipotent mesenchymal cell line (14), MLOY4 osteocytic cell line (15). Lower panel – loading control: ethydium bromide stained membrane.

sible explanation is, that a NADPH-dependent electron donating system, such as a flavoprotein, might interact with AtNOS1 and thus might have been copurified with the AtNOS1 protein from *E. coli*.

What might be the electron donating partner in vivo? Localization of mAtNOS1 in a vicinity of the inner mitochondrial membrane (Fig. 3) might imply interaction with components of mitochondrial electron chain. Indeed, studies in yeast but also in alga, both lacking the classical NOS gene, point to involvement of the mitochondrial electron transport system in NO production [33,34]. In this light, it is tempting to speculate that eukaryotic orthologs of AtNOS1 may link the mitochondrial electron transport system with NO production.

Currently, we are in a process of purification of mAtNOS1, hAtNOS1, and identification of their mitochondrial interaction partners. In addition, generation of a mAtNOS1 knockout mouse will help us to further define the physiological role of this novel candidate for mitochondrial NOS in mammals.

Acknowledgements: T.Z. acknowledges financial support received from BioSapiens Network of Excellence funded by the European Commission within its FP6 Programme, under the thematic area 'Life sciences, genomics and biotechnology for health', contract number LHSG-CT-2003-503265. I.M. and P.M. acknowledge founding from the Ministry of Education, Youth, and Sports of the Czech Republic, Grant 0021620806. P.G. is supported by National Institute on Aging (award AG023264-02) and American Heart Association (award 0565221B). We thank Gerhild Lüder for help with electron microscopy.

Appendix A. Supplementary data

Supplementary data associated with this article can be found, in the online version, at doi:10.1016/j.febslet.2005.12.038.

References

[1] Raman, C.S., Li, H., Martasek, P., Kral, V., Masters, B.S. and Poulos, T.L. (1998) Crystal structure of constitutive endothelial nitric oxide synthase: a paradigm for pterin function involving a novel metal center. Cell 95, 939–950.
[2] Zhang, J., Martasek, P., Paschke, R., Shea, T., Siler Masters, B.S. and Kim, J.J. (2001) Crystal structure of the FAD/NADPH-binding domain of rat neuronal nitric-oxide synthase. Comparisons with NADPH-cytochrome P450 oxidoreductase. J. Biol. Chem. 276, 37506–37513.
[3] Zemojtel, T., Wade, R.C. and Dandekar, T. (2003) In search of the prototype of nitric oxide synthase. FEBS Lett. 554, 1–5.
[4] Panda, K., Ghosh, S. and Stuehr, D.J. (2001) Calmodulin activates intersubunit electron transfer in the neuronal nitric-oxide synthase dimer. J. Biol. Chem. 276, 23349–23356.
[5] Zemojtel, T., Scheele, J.S., Martasek, P., Masters, B.S., Sharma, V.S. and Magde, D. (2003) Role of the interdomain linker probed by kinetics of CO ligation to an endothelial nitric oxide synthase mutant lacking the calmodulin binding peptide (residues 503–517 in bovine). Biochemistry 42, 6500–6506.
[6] Pant, K., Bilwes, A.M., Adak, S., Stuehr, D.J. and Crane, B.R. (2002) Structure of a nitric oxide synthase heme protein from *Bacillus subtilis*. Biochemistry 41, 11071–11079.
[7] Huang, S., Kerschbaum, H.H., Engel, E. and Hermann, A. (1997) Biochemical characterization and histochemical localization of nitric oxide synthase in the nervous system of the snail, *Helix pomatia*. J. Neurochem. 69, 2516–2528.
[8] Guo, F.Q., Okamoto, M. and Crawford, N.M. (2003) Identification of a plant nitric oxide synthase gene involved in hormonal signaling. Science 302, 100–103.
[9] Zemojtel, T., Penzkofer, T., Dandekar, T. and Schultz, J. (2004) A novel conserved family of nitric oxide synthase? Trends Biochem. Sci. 29, 224–226.
[10] Babson, A.L. and Babson, S.R. (1973) Kinetic colorimetric measurement of serum lactate dehydrogenase activity. Clin. Chem. 19, 766–769.
[11] Srere, P.A. (1969) (Lowenstein, J.M., Ed.), Methods in Enzymology, vol. XIII, pp. 3–11, Academic Press, London.
[12] Visel, A., Thaller, C. and Eichele, G. (2004) GenePaint.org: an atlas of gene expression patterns in the mouse embryo. Nucleic Acids Res. 32, D552–D556.
[13] Albrecht, A.N., Schwabe, G.C., Stricker, S., Boddrich, A., Wanker, E.E. and Mundlos, S. (2002) The synpolydactyly homolog (spdh) mutation in the mouse – a defect in patterning and growth of limb cartilage elements. Mech. Dev. 112, 53–67.
[14] Hammen, P.K., Waltner, M., Hahnemann, B., Heard, T.S. and Weiner, H. (1996) The role of positive charges and structural segments in the presequence of rat liver aldehyde dehydrogenase in import into mitochondria. J. Biol. Chem. 271, 21041–21048.
[15] Emanuelsson, O., Nielsen, H., Brunak, S. and von Heijne, G. (2000) Predicting subcellular localization of proteins based on their N-terminal amino acid sequence. J. Mol. Biol. 300, 1005–1016.
[16] Guo, F.Q. and Crawford, N.M. (2005) Arabidopsis nitric oxide synthase1 is targeted to mitochondria and protects against oxidative damage and dark-induced senescence. Plant Cell 17, 3436–3450.
[17] Brookes, P.S. (2004) Mitochondrial nitric oxide synthase. Mitochondrion 3, 187–204.
[18] Ghafourifar, P. and Cadenas, E. (2005) Mitochondrial nitric oxide synthase. Trends Pharmacol. Sci. 26, 190–195.
[19] Lacza, Z. et al. (2005) Mitochondrial NO and reactive nitrogen species production: does mtNOS exist? Nitric Oxide, doi:10.1016/j.niox.2005.05.011.
[20] Bates, T.E., Loesch, A., Burnstock, G. and Clark, J.B. (1995) Immunocytochemical evidence for a mitochondrially located nitric oxide synthase in brain and liver. Biochem. Biophys. Res. Commun. 213, 896–900.
[21] Bates, T.E., Loesch, A., Burnstock, G. and Clark, J.B. (1996) Mitochondrial nitric oxide synthase: a ubiquitous regulator of oxidative phosphorylation? Biochem. Biophys. Res. Commun. 218, 40–44.
[22] Ghafourifar, P. and Richter, C. (1997) Nitric oxide synthase activity in mitochondria. FEBS Lett. 418, 291–296.
[23] Giulivi, C., Poderoso, J.J. and Boveris, A. (1998) Production of nitric oxide by mitochondria. J. Biol. Chem. 273, 11038–11043.
[24] Nisoli, E. et al. (2004) Mitochondrial biogenesis by NO yields functionally active mitochondria in mammals. Proc. Natl. Acad. Sci. USA 101, 16507–16512.
[25] Kobzik, L., Stringer, B., Balligand, J.L., Reid, M.B. and Stamler, J.S. (1995) Endothelial type nitric oxide synthase in skeletal muscle fibers: mitochondrial relationships. Biochem. Biophys. Res. Commun. 211, 375–381.

[26] Gao, S. et al. (2004) Docking of endothelial nitric oxide synthase (eNOS) to the mitochondrial outer membrane: a pentabasic amino acid sequence in the autoinhibitory domain of eNOS targets a proteinase K-cleavable peptide on the cytoplasmic face of mitochondria. J. Biol. Chem. 279, 15968–15974.
[27] Tatoyan, A. and Giulivi, C. (1998) Purification and characterization of a nitric-oxide synthase from rat liver mitochondria. J. Biol. Chem. 273, 11044–11048.
[28] Kanai, A.J., Pearce, L.L., Clemens, P.R., Birder, L.A., VanBibber, M.M., Choi, S.Y., de Groat, W.C. and Peterson, J. (2001) Identification of a neuronal nitric oxide synthase in isolated cardiac mitochondria using electrochemical detection. Proc. Natl. Acad. Sci. USA 98, 14126–14131.
[29] Elfering, S.L., Sarkela, T.M. and Giulivi, C. (2002) Biochemistry of mitochondrial nitric-oxide synthase. J. Biol. Chem. 277, 38079–38086.
[30] Riobo, N.A., Melani, M., Sanjuan, N., Fiszman, M.L., Gravielle, M.C., Carreras, M.C., Cadenas, E. and Poderoso, J.J. (2002) The modulation of mitochondrial nitric-oxide synthase activity in rat brain development. J. Biol. Chem. 277, 42447–42455.
[31] Lacza, Z., Snipes, J.A., Zhang, J., Horvath, E.M., Figueroa, J.P., Szabo, C. and Busija, D.W. (2003) Mitochondrial nitric oxide synthase is not eNOS, nNOS or iNOS. Free Radic. Biol. Med. 35, 1217–1228.
[32] Grishin, N.V. (2001) Treble clef finger – a functionally diverse zinc-binding structural motif. Nucleic Acids Res. 29, 1703–1714.
[33] Cassanova, N., O'Brien, K.M., Stahl, B.T., McClure, T. and Poyton, R.O. (2005) Yeast flavohemoglobin, a nitric oxide oxidoreductase, is located in both the cytosol and the mitochondrial matrix: effects of respiration, anoxia, and the mitochondrial genome on its intracellular level and distribution. J. Biol. Chem. 280, 7645–7653.
[34] Tischner, R., Planchet, E. and Kaiser, W.M. (2004) Mitochondrial electron transport as a source for nitric oxide in the unicellular green alga *Chlorella sorokiniana*. FEBS Lett. 576, 151–155.